Successive DF Relaying: MS-DIS aided Interference Suppression and Three-Stage Concatenated Architecture Design

Li Li, Li Wang, *Member, IEEE* and Lajos Hanzo, *Fellow, IEEE*
School of ECS, University of Southampton, SO17 1BJ, United Kingdom.
Tel: +44-23-8059 3125, Fax: +44-23-8059 4508
Email: {ll5e08, lw05r, lh}@ecs.soton.ac.uk, http://www-mobile.ecs.soton.ac.uk

***Abstract*— Conventional single-relay aided two-phase cooperative networks employing coherent detection algorithms incur a significant 50% throughput loss. Furthermore, it is unrealistic to expect that in addition to the task of relaying, the relay-station would dedicate further precious resources to the estimation of the source-relay channel in support of coherent detection. In order to circumvent these problems, we propose decode-and-forward (DF) based successive relaying employing noncoherent detection schemes. A crucial challenge in this context is that of suppressing the successive relaying induced interference, despite dispensing with any channel state information (CSI). We overcome this challenge by introducing a novel adaptive Newton algorithm based multiple-symbol differential interference suppression (MS-DIS) scheme. Correspondingly, a three-stage concatenated transceiver architecture is devised. We demonstrate that our proposed system is capable of near-error-free transmissions at low signal-to-noise ratios.**

I. Introduction

Coherent detection schemes impose a substantial energy consumption owing to complex and power-hungry channel estimation, which may become prohibitive in Multiple-Input Multiple-Output (MIMO) systems, where numerous channels have to be estimated. Consequently, noncoherent detection scheme dispensing with channel estimation becomes an attractive alternative. Motivated by this rationale, Lampe *et al.* devised a soft-input soft-output multiple-symbol differential sphere detection (SISO-MSDSD) algorithm [1], which is a state-of-the-art noncoherent detection technique.

Due to the limited antenna-separation of shirt-pocket-sized mobiles, the spatial diversity gain promised by MIMO systems [2] was shown to be eroded. By contrast, the family of cooperative techniques heralded by Van Der Meulen [3] is capable of achieving uplink transmit diversity by forming a virtual antenna array (VAA) from the individual single antennas of the mobiles. However, the conventional two-phase cooperative system incurs a severe multiplexing loss due to the half-duplex constraint of practical transceivers. In order to recover the resultant 50% throughput loss, the successive relaying aided network (SRAN) concept was proposed by Fan *et al.* in [4]. Nevertheless, the interference encountered both at the relays and at the destination significantly degrade the benefits of the successive relaying regime.

To the best of our knowledge, the implementation of interference suppression for the SRAN remains an open challenge, when employing noncoherent detection. Additionally, the differential interference suppression (DIS) philosophy was discussed in [5], which was further developed to its multiple-symbol (MS) based version in [6], where a novel amalgam of the adaptive modified Newton algorithm of [7] and of SISO-MSDSD was created.

Hence, our main contributions in this paper are:

1) We conceive successive relaying induced interference suppression at the destination, which is achieved despite dispensing with CSI by incorporating multiple-symbol differential interference suppression (MS-DIS) in SRANs.
2) Consequently, a new adaptive MS-DIS filter and a MSDSD decoder assisted channel-code-aided three-stage turbo decoder is designed for the Base Station's (BS) receiver.

The rest of this paper is organised as follows. Our system model is portrayed in Section II. In Section III, the adaptive MS-DIS scheme is analysed. We design the architecture of the transceiver in Section IV. The performance of the proposed transceiver is characterized in Section V. Finally, we conclude in Section VI.

II. System Model

The topology of a SRAN is depicted in Figure 1, where the Mobile Station s, the activated relay nodes (RN) $r_i, i \in \{0,1\}$ and the destination d are explicitly labelled. Then, we assume that all the channels involved are time-selective Rayleigh fading channels and the notation $\mathbf{H}_{ab}, (a,b) \in \{s, r_0, r_1, d\}$ represents the channel impulse response (CIR) matrix spanning from entity a to b. Furthermore, the relay-aided path-loss reduction [8] is also considered in our system. Accordingly, the path-loss gain of the Source-to-Relay (SR_i) link and Relay-to-Destination (R_iD) link with respect to the Source-to-Destination (SD) link are introduced here as $G_{sr_i} = \{\frac{D_{sd}}{D_{sr_i}}\}^\alpha$ and $G_{r_id} = \{\frac{D_{sd}}{D_{r_id}}\}^\alpha$, respectively, where D_{ab} represents the distance between a and b, while the path-loss exponent α is fixed to 3 here to model a typical urban area. The transmit power of the node a is represented as $P_a, a \in \{s, r_0, r_1\}$. Then we assume that N_t transmit antennas are used both at s, as well as at r_i, while N_r receive antennas are employed at d. Finally, the classic frame-by-frame based transmission having a frame length of L is employed here.

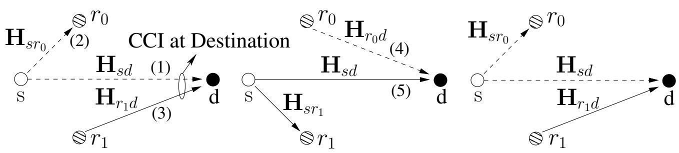

(a) Even Phase (b) Odd Phase (c) Even Phase

Fig. 1: Transmission processes of SRANs.

The transceiver architecture designed for the SRAN is portrayed in Figure 2. For the sake of relating Figure 1 to Figure 2, the same transmissions are numbered by the same indices in the two figures. For example, since the transmissions from the source node (SN) to the destination node (DN) during the "(a) Even Phase" in Figure 1 corresponds to the transmissions from the SN's transmit antenna to the receive antennae of the "Even Phase Multiple-Symbol DIS Filter" in Figure 2, both of them are labelled by the index 1.

The system model corresponding to Figure 1 may be constructed for the k^{th} symbol duration of the l^{th} frame as

$$\mathbf{Y}^l[k] = \sqrt{G_{sd}}\mathbf{S}^l[k]\mathbf{H}^l_{sd}[k] + \sqrt{G_{r_id}}\mathbf{C}^l_{r_i}[k]\mathbf{H}^l_{r_id}[k] + \mathbf{W}^l[k], \quad (1)$$

where the variables $\mathbf{Y}^l[k] \in \mathbb{C}^{N_t \times N_r}$, $\mathbf{S}^l[k] \in \mathbb{C}^{N_t \times N_t}$, $\mathbf{C}^l_i[k] \in \mathbb{C}^{N_t \times N_t}$, $\mathbf{H}^l_{ab}[k] \in \mathbb{C}^{N_t \times N_r}$, and $\mathbf{W}^l[k] \in \mathbb{C}^{N_t \times N_r}$ denote the k^{th}

The financial support of the European Union under the auspices of the Concerto project, as well as that of the RC-UK under the auspices of the India-UK Advanced Technology Centre known as IN-ATC is gratefully acknowledged.

signal matrix received at the DN, the SN's broadcast symbol matrix, the RN's forwarded symbol matrix, the associated CIR matrix, and the AWGN matrix obeying a distribution of $\mathcal{CN}(0, 2\delta_w^2)$, respectively. The subscript i involved in (1) is calculated as $i = \mathrm{mod}_2(l+1)$ and $l = 0, 1, \cdots$. Since the above-mentioned MS-DIS regime will be employed in our system, it is necessary to extend the symbol-by-symbol based system model characterized by (1) to its multiple-symbol based version. Accordingly, the n^{th} signal block matrix received during the l^{th} frame may be readily formulated as

$$\underline{\mathbf{Y}}^l[n] = \sqrt{G_{sd}}\underline{\mathbf{S}}^l[n]\underline{\mathbf{H}}_{sd}^l[n] + \sqrt{G_{r_id}}\underline{\mathbf{C}}_{r_i}^l[n]\underline{\mathbf{H}}_{r_id}^l[n] + \underline{\mathbf{W}}^l[n], \quad (2)$$

where $\underline{\mathbf{Y}}^l[n]$ consists of N_{wind} consecutively received $\mathbf{Y}^l[k]$ contributions obeying the form of

$$\underline{\mathbf{Y}}^l[n] = \begin{bmatrix} \mathbf{Y}^l[L\cdot l + (N_{wind}-1)\cdot n] \\ \vdots \\ \mathbf{Y}^l[L\cdot l + (N_{wind}-1)\cdot (n+1)] \end{bmatrix}. \quad (3)$$

Then the CIR block $\underline{H}_{ab}^l[n]$ as well as the AWGN block $\underline{W}^l[n]$ are constructed by vertically stacking the associated $\mathbf{H}_{ab}^l[k]$ and $\mathbf{W}^l[k]$ matrices in a form similar to (3), respectively. Furthermore, the n^{th} SN broadcast symbol block is given by $\underline{\mathbf{S}}^l[n] = diag\{[\mathbf{S}^l[L\cdot l + (N_{wind}-1)\cdot n]^T, \cdots, \mathbf{S}^l[L\cdot l + (N_{wind}-1)\cdot(n+1)]^T]^T\}$. An $\mathcal{M}$-ary differential encoding scheme is employed here, hence we have $\mathbf{S}^l[k+1] = \mathbf{S}^l[k]\mathbf{V}^l[k]$ and $\underline{\mathbf{S}}^l[n]$ will be uniquely determined by the length-$(N_{wind}-1)$ information symbol block matrix $\underline{\mathbf{V}}^l[n] = [\mathbf{V}^l[L\cdot l + (N_{wind}-1)\cdot n]^T, \cdots, \mathbf{V}^l[L\cdot l + (N_{wind}-1)\cdot(n+1)-1]^T]^T$.

The decode-and-forward (DF) relaying protocol is employed at the RN. If the RN perfectly detects the received information bits and re-encodes, as well as re-modulates them in the same way as the SN, we arrive at

$$\underline{\mathbf{C}}_{r_i}^l[n] = \underline{\mathbf{S}}^{l-1}[n]. \quad (4)$$

III. Adaptive Multiple-Symbol Based Differential Interference Suppression

It is revealed by (2) that the transmitted signals of the SN and RN always interfere with each other at the DN. The associated co-channel interference (CCI) is also illustrated in Figure 1, where transmission-3 and transmission-5 will contaminate the DN's signals received due to transmission-1 and transmission-4, respectively. Hence noncoherent detection cannot be directly applied at the DN, before an interference suppression stage is invoked at the input of the DN receiver. When we want to detect the signal received from the SN, the first term of (2) becomes the desired signal component, while the remaining terms represent the interference-plus-noise component. This partitioning of the received signal block matrix $\underline{\mathbf{Y}}^l[n]$ is detailed as

$$\underline{\mathbf{Y}}^l[n] = \underbrace{\sqrt{G_{sd}}\underline{\mathbf{S}}^l[n]\underline{\mathbf{H}}_{sd}^l[n]}_{\text{desired component}} + \underbrace{\sqrt{G_{r_id}}\underline{\mathbf{C}}_{r_i}^l[n]\underline{\mathbf{H}}_{r_id}^l[n] + \underline{\mathbf{W}}^l[n]}_{\text{interference-plus-noise component}}. \quad (5)$$

In order to extract the N_{wind} differentially encoded symbols pertaining to the desired signal component from the complete received signal block matrix $\underline{\mathbf{Y}}^l[n]$, $\underline{\mathbf{Y}}^l[n]$ can be passed through an adaptive filter having the coefficient vector $\boldsymbol{f}_g$ of length N_r for the sake of suppressing the interference-plus-noise component. The filter output is given by

$$\mathbf{y}_g^l[n] = \underline{\mathbf{Y}}^l[n]\boldsymbol{f}_g. \quad (6)$$

Based on the maximum signal-to-interference-plus-noise ratio (MSINR) criterion [5], the optimum coefficient vector $\boldsymbol{f}_g$, which is capable of maximising the filter's output SINR is given by

$$\boldsymbol{f}_g = \max_{\boldsymbol{f}_g} \frac{\boldsymbol{f}_g^H(\mathbf{R}_{rr} - \mathbf{R}_{ee})\boldsymbol{f}_g}{\boldsymbol{f}_g^H\mathbf{R}_{ee}\boldsymbol{f}_g} = \max_{\boldsymbol{f}_g} \frac{\boldsymbol{f}_g^H\mathbf{R}_{rr}\boldsymbol{f}_g}{\boldsymbol{f}_g^H\mathbf{R}_{ee}\boldsymbol{f}_g}, \quad (7)$$

where the correlation matrix of the entire received signal block and of the interference-plus-noise component are defined by

$$\mathbf{R}_{rr} \triangleq \left(\sum_{ab\in sd, r_id} \underline{\mathbf{H}}_{ab}^{l\ H}[n]\underline{\mathbf{H}}_{ab}^l[n]\right) + N_tN_{wind}2\delta_w^2\mathbf{I}_{N_r}, \quad (8)$$

$$\mathbf{R}_{ee} \triangleq \underline{\mathbf{H}}_{r_id}^{l\ H}[n]\underline{\mathbf{H}}_{r_id}^l[n] + N_tN_{wind}2\delta_w^2\mathbf{I}_{N_r}, \quad (9)$$

respectively. Then $\mathbf{I}_{N_r}$ represents an identity matrix having $(N_r \times N_r)$ elements. Furthermore, $[\cdot]^H$ denote the Hermitian transposition.

However, according to (8) and (9), the CIR block matrix $\underline{\mathbf{H}}_{ab}^l[n]$ has to be known by the receiver for the sake of calculating the correlation matrices $\mathbf{R}_{rr}$ and $\mathbf{R}_{ee}$, which inherently conflicts with the employment of noncoherent detection. Then, even through the receiver already acquired the CIR block matrix $\underline{\mathbf{H}}_{ab}^l[n]$, we have to utilize the singular-value decomposition (SVD) [9] to implement the generalized eigen-decomposition for solving (7), which usually imposes a high computational complexity.

In order to circumvent above problems, the adaptive modified Newton algorithm is proposed here, which was shown in [7] to have a fast convergence and an excellent tracking capability. This scheme was further developed to its multiple-symbol based version in [6]. For reasons of space economy, the major steps of implementing the adaptive modified Newton algorithm are directly summarized as

$$\begin{aligned}
\mathbf{P}[n] &= \frac{\mathbf{P}[n-1]}{\mu}\left(\mathbf{I}_{N_r} - \frac{\underline{\mathbf{E}}_g^{l\ H}[n]\underline{\mathbf{E}}_g^l[n]\mathbf{P}[n-1]}{\mathrm{tr}\left(\mu\mathbf{I}_{N_r} + \underline{\mathbf{E}}_g^l[n]\mathbf{P}[n-1]\underline{\mathbf{E}}_g^{l\ H}[n]\right)}\right) \\
\mathbf{c}[n] &= \underline{\mathbf{Y}}^l[n]\boldsymbol{f}_g[n-1], \\
\mathbf{r}[n] &= \beta\mathbf{r}[n-1] + (1-\beta)\underline{\mathbf{Y}}^{l^H}[n]\mathbf{c}[n], \\
d[n] &= \beta d[n-1] + (1-\beta)\mathbf{c}^H[n]\mathbf{c}[n], \\
\tilde{\boldsymbol{f}}_g[n] &= \frac{\mathbf{r}[n]}{d[n]}, \\
\boldsymbol{f}_g[n] &= \frac{2\mathbf{P}[n]\tilde{\boldsymbol{f}}_g[n]}{1 + \tilde{\boldsymbol{f}}_g^H[n]\mathbf{P}[n]\tilde{\boldsymbol{f}}_g[n]},
\end{aligned} \quad (10)$$

where $0 \le \beta, \mu \le 1$ are the forgetting factors. Then, the initialization of the associated parameters is implemented as: set $\mathbf{P}[0] = \mu_1\mathbf{I}_{N_r}$, $\boldsymbol{f}_g[0] = \mathbf{r}[0] = \mu_2[1, 1, \cdots, 1]^T$ and $d[0] = \mu_3$, where $\mu_i(i = 1, 2, 3)$ are appropriate positive values. Moreover, similar to [5, (11)], by exploiting the differential encoding principle, the multiple-symbol-based error signal block matrix $\underline{\mathbf{E}}_g^l[n]$ involved in (10) may be expressed as

$$\underline{\mathbf{E}}_g^l[n] = \sqrt{\frac{1}{2}}\left(\underline{\mathbf{Y}}^l[n] - \underline{\hat{\mathbf{V}}}_g^l[n] \cdot \underline{\mathbf{Y}}^l[\overleftarrow{n}^{(1)}]\right), \quad (11)$$

where the operation "$\cdot$" denotes the submatrix-wise multiplication between two matrices. Then the specific block index $\overleftarrow{n}^{(m)}$ represents the n^{th} signal block, which was shifted backwards by m symbol durations. Furthermore, $\underline{\hat{\mathbf{V}}}_g^l[n] = [\mathbf{V}^l[L\cdot l + (N_{wind}-1)\cdot n - 1]^T, \underline{\mathbf{V}}^l[n]^T]^T$ is the n^{th} transmitted information symbol block corresponding to the desired component of (5), which determined by the training block of the adaptive filter or it is actually substituted by the previous decisions in the decision-directed model of the adaptive filter. The reliability of the temporary decisions made during the decision-directed filter adaptation dominate the performance of the adaptive MS-DIS filter. In order to improve their reliability, we employ the Relay-Aided SISO-MSDSD algorithm of [10], which requires the further development of the SISO-MSDSD algorithm for simultaneously detecting multiple input signal streams, where the multiple input signal streams were expected to correspond to the same modulated symbols.

The adaptive filter coefficient vector $\boldsymbol{f}_g[n]$ conditioned for extracting the differentially encoded symbols pertaining to the SN's broadcast signals is denoted by $\boldsymbol{f}_s[n]$. Then, $\boldsymbol{f}_g[n]$, which was specifically adjusted for extracting the differentially encoded symbols pertaining to the RN's forwarded signals is denoted by $\boldsymbol{f}_{r_i}[n]$. Assuming the validity of (4) and substituting (4) into (2), the two received signal blocks having the same block index n but two different frame indices of l and $(l+1)$ can be further formulated as

$$\underline{\mathbf{Y}}^l[n] = \sqrt{G_{sd}}\underline{\mathbf{S}}^l[n]\underline{\mathbf{H}}_{sd}^l[n] + \underline{\mathbf{I}}^l[n] + \underline{\mathbf{W}}^l[n],$$
$$\underline{\mathbf{Y}}^{l+1}[n] = \sqrt{G_{r_id}}\underline{\mathbf{S}}^l[n]\underline{\mathbf{H}}_{r_id}^{l+1}[n] + \underline{\mathbf{I}}^{l+1}[n] + \underline{\mathbf{W}}^{l+1}[n], \qquad (12)$$

where $\underline{\mathbf{I}}^l[n]$ represents the associated interference component.

After $\underline{\mathbf{Y}}^l[n]$ and $\underline{\mathbf{Y}}^{l+1}[n]$ are passed through the adaptive filter and multiplied by $\boldsymbol{f}_s[n]$ and $\boldsymbol{f}_{r_i}[n]$, respectively, the filter outputs are given by

$$\mathbf{y}_s^l[n] = \underline{\mathbf{Y}}^l[n]\boldsymbol{f}_s[n]$$
$$\mathbf{y}_{r_i}^{l+1}[n] = \underline{\mathbf{Y}}^{l+1}[n]\boldsymbol{f}_{r_i}[n]. \qquad (13)$$

Both $\mathbf{y}_s^l[n]$ and $\mathbf{y}_{r_i}^{l+1}[n]$ correspond to the differentially encoded symbol block $\underline{\mathbf{S}}^l[n]$. Hence the basic condition to be met for the sake of utilizing the Relay-Aided SISO-MSDSD algorithm is satisfied. Consequently, we substitute $\mathbf{y}_s^l[n]$ and $\mathbf{y}_{r_i}^{l+1}[n]$ into [10, (8)] as the multiple input signal streams. By implementing the Relay-Aided SISO-MSDSD, the temporary decisions $\hat{\underline{\mathbf{V}}}_g^l[n]$ in (11) can be acquired [1].

Hence, the adaptive filter coefficient vector $\boldsymbol{f}_g[n]$ can be approximated and updated by recursively implementing the procedure of (10) on a block-by-block basis. Consequently, the suppression of the interference-plus-noise component dispensing with CSI becomes possible.

IV. Transceiver Design and Analysis

We specifically design a transceiver for the proposed DF aided SRAN, which implements the state-of-the-art techniques introduced in Section III and efficiently organizes the collaboration amongst all functional blocks. The transceiver architecture is portrayed in Figure 2.

A. Architecture Design

In order to enhance the error correction capability of the decoder, channel coding is invoked as an essential part of contemporary communication systems. Since it was demonstrated in [11] that Self-Concatenated Convolutional Codes (SECCC) [12] are capable of outperforming state-of-the-art benchmarks, instead of the most frequently employed schemes, e.g. the Recursive Systematic Convolution (RSC) code, a SECCC encoder is employed as the outer code at the SN. Then, the SECCC is combined with a differentially encoded modulator, which is further amalgamated with a unity-rate-code (URC) in order to create a two-stage inner code. Consequently, a three-stage SECCC-URC-DM source encoder was conceived.

As seen in Figure 2, a symmetric iterative decoder is employed at the RN, which consists of three components, namely the SISO-MSDSD decoder, the URC decoder and the SECCC decoder[2]. In Figure 2 the notations $E(\cdot)$ and $A(\cdot)$ denote the *extrinsic* information and *a priori* information, respectively, which are iteratively interleaved and exchanged I_{inner}^r times within the two-stage MSDSD-URC inner code and then passed on to the SECCC outer code. The resultant signal will be further iteratively exchanged I_{outer}^r times between the inner MSDSD-URC code and the outer SECCC code. The URC model has an IIR as a benefit of its recursive encoder structure. Hence it is capable of meritoriously reshaping the EXIT curve of the two-stage inner code to approach the point of perfect convergence at $(1, 1)$ in the EXIT chart, which implies that an infinitesimally low error probability is attained. Consequently, a potentially critical impediment of the DF protocol, namely its error propagation may be avoided and (4) is satisfied. The transmitter of the RN may be designed to obey exactly the same architecture as that of the SN.

Since the Base Station (BS) can typically afford a higher system complexity and energy consumption, the proposed adaptive interference suppression procedure maybe readily invoked at the BS. Relying on the analysis of Section III and still focusing on the detection of the information pertaining to the SN's broadcast signals during the even-indexed transmission phase, the MS-DIS filter is configured to employ the appropriate coefficient vector $\boldsymbol{f}_s[n]$. After passing the received signal block matrix $\underline{\mathbf{Y}}^l[n]$ of (12) to the MS-DIS filter of the even-phase, the filter output $\mathbf{y}_s^l[n]$ of (13) is attained. Then, another replica of the differentially encoded symbol block $\underline{\mathbf{S}}^l[n]$ of (5) pertains to the RN's forwarded signal block having the block index n and frame index $(l+1)$. Hence the MS-DIS filter of the consecutive odd-phase should be configured to use the coefficient vector $\boldsymbol{f}_{r_i}[n]$ and to generate the corresponding filter output $\mathbf{y}_{r_i}^{l+1}[n]$ of (13). These operations are explicitly portrayed within the "Destination" block of Figure 2[3]. In order to simultaneously decode $\mathbf{y}_s^l[n]$ and $\mathbf{y}_{r_i}^{l+1}[n]$, the MS-DIS filter is concatenated with the Relay-Aided SISO-MSDSD decoder as proposed in Section III. The remaining architectural features of our BS receiver are constituted by the URC decoder and the SECCC decoder, which are arranged similarly to the corresponding part of the RN's receiver.

B. Turbo Equalization Based Decoding Regime

The turbo equalization philosophy was originally proposed in [14] and detailed in [15]. As a benefit of the gradually increased reliability of the feedback decisions, the performance of the turbo equalizer may be significantly improved upon increasing the number of iterations. Hence we configure the MS-DIS filter iteratively process the same received signal frame a number of times with the aid of the most recent feedback decisions in each and every inner iteration of the two-stage MSDSD-URC inner code. As proposed in [6], the soft-symbol-decision-directed feedback philosophy is adopted and the coefficient vector $\boldsymbol{f}_g[n]$ is updated on a block-by-block basis to reduce the complexity imposed. For the sake of appropriately adjusting the coefficients of the adaptive equalizer, a training sequence constituted by legitimate differentially encoded symbols and known a priori by the DN is periodically transmitted by the SN according to the affordable training overhead. Hence, in the training mode, the MS-DIS filter exploits the knowledge of the training symbols to adapt its coefficient vector. Then, in the decision-directed mode, both the *extrinsic* information generated by the relay-aided MSDSD decoder in the last iteration and the *a priori* information provided

[1]For the further derivations and interpretation of the Relay-Aided SISO-MSDSD algorithm we refer to [10]

[2]Our motivation of employing this three-stage rather than two-stage concatenated architecture is to improve the convergence behaviour of the iterative decoder with the aid of the URC decoder, as heralded in [13].

[3]Actually, only one antenna array and one MS-DIS filter are activated at the beginning of the DN's action. The explicitly displayed dual antenna arrays and two MS-DIS filters are used to emphasize the distinctive nature of the even and odd phases. Hence the antenna array and the MS-DIS filter corresponding to the odd phase are represented by dashed lines.

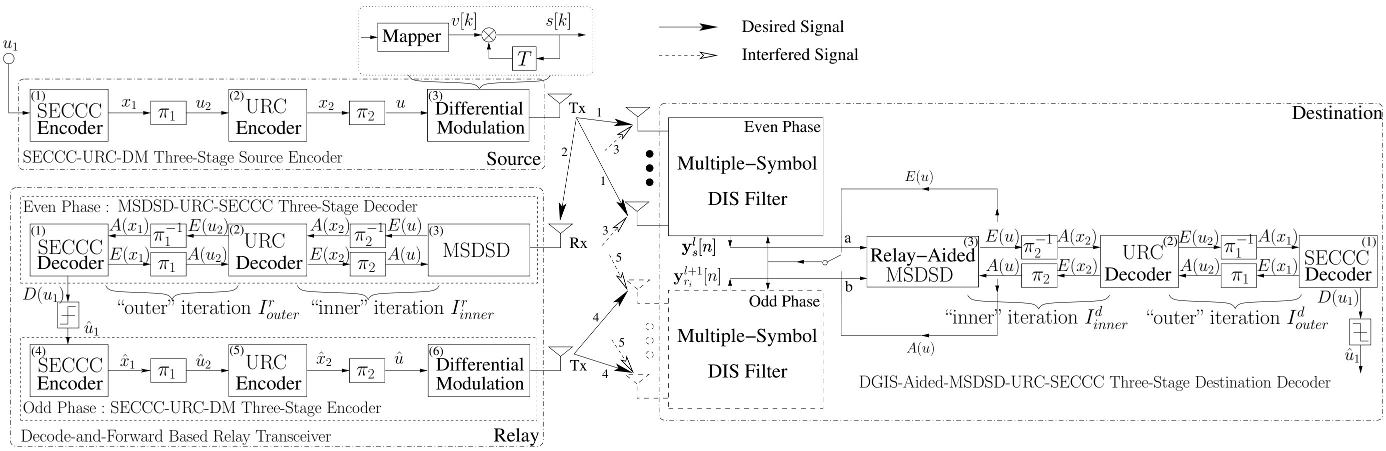

Fig. 2: The architecture of our proposed MS-DIS plus MSDSD assisted SECCC aided three-stage turbo transceiver

by the URC decoder in the present iteration may be utilized as the soft decision feedback for updating the coefficient vector. Hence, a supplemental comparison between the *extrinsic* information and the *a priori* information is needed, so that the higher one may be invoked.

In more detail, during the first inner iteration, i.e for $I^d_{inner} = 1, I^d_{outer} = 1$, the MS-DIS filter initially invokes the current coefficient vector for suppressing the interference and then updates its coefficient vector based on the current feedback decisions. This implies that the coefficient vector generated during the n^{th} block is actually only utilized during the $(n+1)^{st}$ block. Furthermore, in this iteration, the switch shown in Figure 2 should be set to point "a", since the *a priori* information provided by the URC decoder equals to zero. During the consecutive iterations, the MS-DIS filter will first update its coefficient vector based on the feedback decisions generated during the most recent iteration and then utilizes the updated coefficient vector to suppress the interference. Meanwhile the switch will oscillate between the points "a" and "b".

V. Simulation Results and Discussions

Normalized Doppler Frequency	$f_d = 0.01$
Relay Position	$D_{sr_i} = \frac{1}{2}$; $G_{sr_i} = G_{r_id} = 8$
Channel Coding	SECCC
Memory Length of SECCC	$\nu = 6$
Puncture Rate of SECCC	$p = 0.5$
Iteration Number of SECCC	$I_{SECCC} = 2$
Code Rate of SECCC	$R_c = 0.5$
Interleaver Length	$L = 144000$ bits
Modulation	DQPSK
MSDSD Observation Window Size	$N_{wind} = 6$
Overall Bandwidth efficiency	$\eta \approx \frac{T_b-1}{T_b} R_c \log_2 M_c = 0.83$ bit/s/Hz
Optimum Forgetting Factor	$\beta = 0.995; \mu = 0.30$
Training Overhead	2%
Initialization of MS-DIS Filter	$\mu_1 = 0.01; \mu_2 = \frac{1}{\sqrt{\|\boldsymbol{f}_g[n]\|_F^2}}; \mu_3 = 1$
Antenna Configuration	$N_t = 1$; $N_r = 4$

TABLE I: SYSTEM PARAMETERS

Let us now report on our experiments, including the effects of the forgetting factors (β, μ), and the error correction capability of both the RN's and the BS's receiver. The major system parameters adopted in our simulations are summarized in Table I.

The specific choice of the forgetting factors (β, μ) invoked in Section III significantly influences the performance of the adaptive modified Newton algorithm, as mentioned in [7]. Hence finding the optimum forgetting factors associated with a specific scenario is required. It was shown in [16] that the area under the bit-based EXIT curve of the inner code approximates the maximum achievable coding rate of the outer channel code, while guaranteeing near-error-free communication. Hence we can utilize the EXIT curves of the

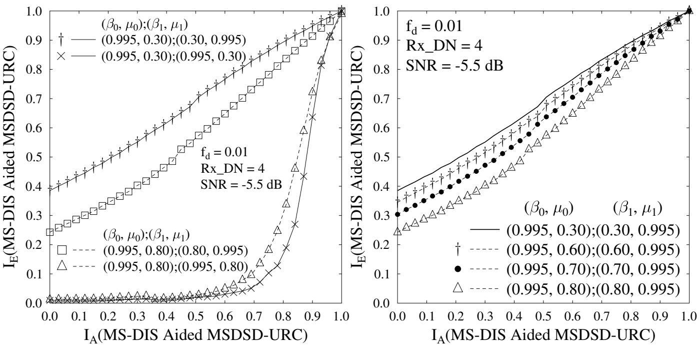

(a) Forgetting factor comparison-I (b) Forgetting factor comparison-II

Fig. 3: EXIT-curve-assisted forgetting factor optimization.

MS-DIS aided MSDSD-URC inner codes having different forgetting factor values to solve the corresponding optimization problem. Consequently, the EXIT curve assisted optimization of the forgetting factors is supported by the relevant results shown in Figure 3.

The forgetting factors involved in the MS-DIS filters of the even and odd phases are represented by (β_0, μ_0) and (β_1, μ_1), respectively. Due to the particular transmission regime of the SRAN, when focusing on the detection of a differentially encoded symbol block $\underline{\mathbf{S}}^l[n]$, the roles of the associated signal components received by the DN from the SN and RN are reversed in the consecutive even and odd phases in terms of the desired component and the interference-plus-noise component. Hence, according to the functions[4] of the forgetting factors β and μ, it may be readily inferred that the values of (β_0, μ_0) and (β_1, μ_1) should also obey a reversed relationship, in order to realize a reasonable collaboration between the even-phase MS-DIS filter and odd-phase MS-DIS filter. This statement is verified by Figure 3a, where the EXIT curves corresponding to the forgetting factors satisfying "$\beta_1 = \beta_0; \mu_1 = \mu_0$" are shifted further down compared to the forgetting factors obeying "$\beta_1 = \mu_0; \mu_1 = \beta_0$". After confirming the optimization rule that "$\beta_1 = \mu_0, \mu_1 = \beta_0$", a deeper search and the relevant results are displayed in Figure 3b. Observe in Figure 3b that the area under the EXIT curve of the MS-DIS aided MSDSD-URC inner code was consistently increased upon reducing the value of μ_0, until μ_0 gets close to 0.30. Additionally, our results not included here for space economy also demonstrate that higher β_0 values result in an improved EXIT characteristic. Hence the forgetting factors of $(\beta_0, \mu_0) = (0.995, 0.30)$ were deemed to be the best choice and were employed for the actual MS-DIS filter in our

[4]As detailed in [7], β and μ are invoked to smoothly track $\mathbf{R}_{rr}$ of (8) and $\mathbf{R}_{ee}$ of (9), respectively.

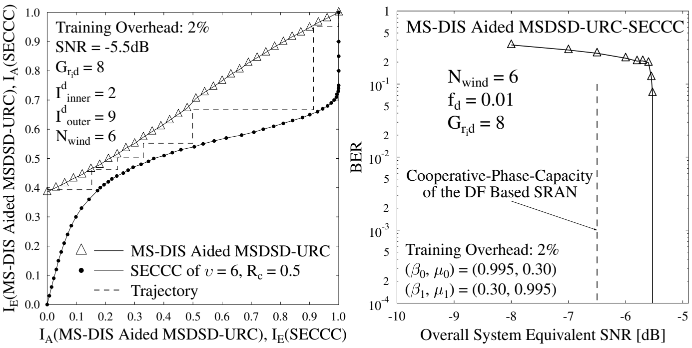

(a) EXIT characteristics (b) BER vs SNR performance

Fig. 4: Error correction performance of the DN.

specific scenario.

Since the BS is capable of supporting a more sophisticated, but higher-complexity architecture than the relays, the number of BS receiver antennae is fixed to $N_r = 4$ for enhancing its diversity gain and hence the attainable error correction capability. Then, in order to concentrate our attention on the DN's characteristics, we stipulate the idealized simplifying assumption that the relays always achieve perfect detection. Based on this assumption, the EXIT chart and the BER vs SNR performance of the proposed BS receiver are portrayed in Figure 4. Observe in Figure 4a that the Monte-Carlo simulation based EXIT-trajectory of the MS-DIS aided MSDSD-URC-SECCC BS receiver is capable of approaching the point of perfect convergence at $(1, 1)$ after $I^d_{outer} = 9$ outer iterations, when the SNR is as low as -5.5dB. It is verified again in Figure 4b that the BER rapidly drops to an infinitesimally low value, when the SNR exceeds -5.5dB. A 2% training overhead was found to be sufficient for adapting the MS-DIS filter in the time-selective fading channel associated with a normalized Doppler frequency of $f_d = 0.01$. Moreover, it is demonstrated in Figure 4b that the proposed BS receiver of Figure 2 attains a performance within about 1.0dB of the corresponding SRAN's cooperative-phase capacity, where the capacity was evaluated according to [10].

The idealized simplifying assumption that the relay perfectly decodes the SN's transmitted signals is verified with the aid of Figure 5. Owing to the compact dimensions of the mobile, the number of relay

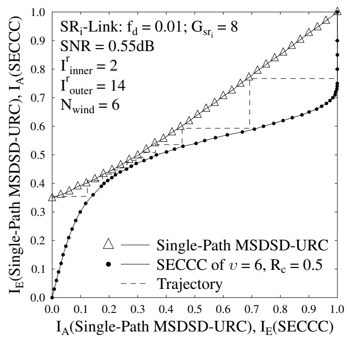

Fig. 5: EXIT chart characteristics at the RN.

receiver antennae is fixed to $N_r = 1$. Observe in Figure 5 that the SNR value has to be above 0.55dB in order to allow the decoding trajectory of the proposed single-path MSDSD-URC-SECCC relay decoder to approach the point of perfect convergence at $(1, 1)$ in the EXIT Chart, even when assuming that the RN does not incur any interference. This implies that the error correction capability of our BS receiver may be significantly impaired by the potential error propagation encountered at the RN. Hence the system operating in a realistic scenario is unable to exhibit an infinitesimally low BER at SNR values as low as -5.5dB. However, the potentially poor error correction capability of the RN's receiver can be improved by introducing an efficient cooperative-user-selection scheme, or by invoking sophisticated power-allocation and code-rate-optimization schemes, which will be addressed in our future research.

VI. CONCLUSIONS

A novel adaptive Newton algorithm based MS-DIS filter was incorporated in the SRAN considered for the suppression of the successive relaying-induced interference. The carefully designed MS-DIS aided MSDSD-URC-SECCC BS receiver exhibited a powerful error correction capability. These novel design contributions improved the practicality of our low-complexity noncoherent detection based SRAN. The relay receiver's poor error correction capability and the issues of inter-relay interference suppression remain open problems, which are hence set aside for our future research.

REFERENCES

[1] V. Pauli, L. Lampe, and R. Schober, ""Turbo DPSK" Using Soft Multiple-Symbol Differential Sphere Decoding," *IEEE Transactions on Information Theory*, vol. 52, pp. 1385–1398, April 2006.

[2] G. J. Foschini and M. J. Gans, "On Limits of Wireless Communications in a Fading Environment when Using Multiple Antennas," *Wireless Personal Communications*, vol. 6, pp. 311–335, Mar 1998.

[3] E. C. van der Meulen, "Three-Terminal Communication Channels," *Advanced Applied Probability*, vol. 3, pp. 120–154, 1971.

[4] Y. Fan, C. Wang, J. Thompson, H. V. Poor, "Recovering Multiplexing Loss through Successive Relaying Using Repetition Coding," *IEEE Transactions on Communications*, vol. 6, pp. 4484–4493, December 2007.

[5] S. K. Cheung and R. Schober, "Differential Spatial Multiplexing," *IEEE Transactions on Wireless Communications*, vol. 5, pp. 2127–2135, Aug 2006.

[6] L. Wang and L. Hanzo, "Multiple-Symbol Detection Aided Differential Spatial Division Multiple Access," *in ICC 2011, Kyoto*, pp. 1–5, June 2011.

[7] J. Yang, F. Yang, H. S. Xi and W. Guo, "Robust Adaptive Modified Newton Algorithm for Generalized Eigendecomposition and Its Application," *EURASIP Journal on Advances in Signal Processing*, vol. 2007, pp. 1–10, Jun 2007.

[8] H. Ochiai, P. Mitran, and V. Tarokh, "Design and Analysis of Collaborative Diversity Protocols for Wireless Sensor Networks," *Vehicular Technology Conference, Los Angeles, CA*, vol. 7, pp. 4645–4649, Sept 2004.

[9] S. Haykin, "Adaptive Filter Theory," *3rd ed. Englewood Cliffs, NJ: Prentice -Hall*, 1996.

[10] L. Li L. Wang and L. Hanzo, "The Capacity of Successive DF Relaying and Using Soft Multiple-Symbol Differential Sphere Detection," *IEEE Globecom 2011*, December 2011, Houston, USA, http://eprints.ecs.soton.ac.uk/22563/.

[11] M. F. Butt, R. Riaz, S. X. Ng and L. Hanzo, "Near-Capacity Iterative Decoding of Binary Self-Concatenated Codes Using Soft Decision Demapping and 3-D EXIT Charts," *IEEE Transactions on Wireless Communications*, vol. 9, pp. 1608–1616, May 2010.

[12] S. Benedetto, D. Divsalar, G. Montorsi, and F. Pollara, "Self-Concatenated Trellis Coded Modulation with Self-Iterative Decoding," *Proc. IEEE Global Telecommunications Conference, Sydney, NSW, Australia*, vol. 1, pp. 585–591, Nov 1998.

[13] D. Divsalar, S. Dolinar, and F. Pollara, "Serial Concatenated Trellis Coded Modulation with Rate-1 Inner Code," *Proc. IEEE Global Telecommunications Conference*, vol. 2, pp. 777–782, Nov 2000.

[14] C. Douillard, A. Picart, P. Didier, M. Jezequel, C. Berrou and A. Glavieux, "Iterative Correction of Intersymbol Interference: Turbo-Equalization," *European Transactions on Telecommunications*, vol. 6, pp. 507–511, Sept 1995.

[15] L. Hanzo, T. H. Liew, B. L. Yeap and R. Y. S. Tee, "Turbo Coding, Turbo Equalisation and Space-Time Coding : EXIT-Chart Aided Near-Capacity Designs for Wireless Channels," *John Wiley & Sons and IEEE Press*, March 2011.

[16] I. Land, S. Huettinger, P. A. Hoeher, and J. B. Huber, "Bounds on Information Combining," *IEEE Transactions on Information Theory*, vol. 51, pp. 612–619, Feb 2005.